SLAC-PUB-11071
April 2005

Design and Performance of Soft Gamma-ray Detector for NeXT Mission

H. Tajima, T. Kamae, G. Madejski
KIPAC/SLAC, Stanford, CA 94025, USA
T. Takahashi, K. Nakazawa, S. Watanabe, T. Mitani, T. Tanaka
Institute of Space and Astronautical Science, Kanagawa 229-8510, Japan
Y. Fukazawa
Hiroshima University, Higashi-Hiroshima, Hiroshima 739-8526, Japan
J. Kataoka, T. Ikagawa
Tokyo Institute of Technology, Meguro-ku, Tokyo,152-8551, Japan
M. Kokubun, K. Makishima
University of Tokyo, Bunkyo-ku, Tokyo 113-0033, Japan
Y. Terada
RIKEN, Wako, Saitama 351-0198, Japan
M. Nomachi
Osaka University, Toyonaka, Osaka 560, Japan
M. Tashiro
Saitama University, Saitama, Saitama 338-8570, Japan

The Soft Gamma-ray Detector (SGD) on board NeXT (Japanese future high energy astrophysics mission) is a Compton telescope with narrow field of view, which utilizes Compton kinematics to enhance its background rejection capabilities. It is realized as a hybrid semiconductor gamma-ray detector which consists of silicon and Cadmium Telluride (CdTe) detectors. It can detect photons in an energy band 0.05–1 MeV at a background level of 5×10^{-7} counts/s/cm^2/keV; the silicon layers are required to improve the performance at a lower energy band (<0.3 MeV). Excellent energy resolution is the key feature of the SGD to achieve both high angular resolution and good background rejection capability. Its ability to measure gamma-ray polarization opens up a new window to study gamma-ray emission in the universe. We will present the development of key technologies to realize the SGD; high quality CdTe, low noise front-end VLSI and bump bonding technology. Energy resolutions of 1.7 keV (FWHM) for CdTe pixel detectors and 1.1 keV for silicon strip detectors have been measured. We also present the validation of Monte Carlo simulation used to evaluate the performance of the SGD.

1. Introduction

The hard X-ray and gamma-ray bands have long been recognized as important windows for exploring the energetic universe. It is in these energy bands that non-thermal emission, primarily due to accelerated high energy particles, becomes dominant. However, by comparison with the soft X-ray band, where the spectacular data from the XMM-Newton and Chandra satellites are revolutionizing our understanding of the high-energy Universe, the sensitivities of hard X-ray missions flown so far, or currently under construction, have not dramatically improved over the last decade. Clearly, the scope of discovery expected with much improved sensitivity for both point and extended sources is enormous.

Recently, a new semiconductor detector based on Cadmium Telluride (CdTe) emerged as a promising detector technology for detection of MeV gamma-rays [1, 2]. Taking advantage of significant progress in CdTe technologies, we are developing a new generation of Compton telescopes, the SGD (Soft Gamma-ray Detector) [3] to be deployed onboard the NeXT (New X-ray Telescope) mission [4] proposed at ISAS (Institute of Space and Astronautical Science) as a successor of the Astro-E2.

The NeXT/SGD is a hybrid semiconductor gamma-ray instrument which consists of silicon and CdTe sensors to detect photons in a wide energy band (0.05–1 MeV); the silicon layers are required to improve the performance at a lower energy band (<0.3 MeV). The silicon layers also improve the angular resolution because of smaller effect of the finite momentum of the Compton-scattering electrons (Doppler broadening) than CdTe. The SGD is a narrow FOV (field-of-view) instrument which utilizes a Compton kinematics telescope to enhance its background rejection capabilities to achieve very low background (5×10^{-7} counts/s/cm^2/keV) [1]. Figure 1 (a) shows expected SGD sensitivities for continuum emission from point source, assuming an observation time of 100 ks and comparison with other instruments [3]. It is evident that the SGD presents great improvement in the soft gamma-ray band. The Compton kinematics rely on the excellent energy resolution afforded by the detector material in the SGD module. This resolution (better than 1.5 keV @ 60 keV) allows the instrument to achieve both high angular resolution and good background rejection capability. As a natural consequence of the Compton approach used to decrease backgrounds, the SGD module is quite sensitive to X/γ-ray polarization, thereby opening up a new window to study particle acceleration and radiation mechanism in astronomical objects.

Submitted to 22nd Texas Symposium On Relativistic Astrophysics At Stanford University, 12/13-12/17/2004, Stanford, CA, USA

Work supported in part by the Department of Energy contract DE-AC02-76SF00515

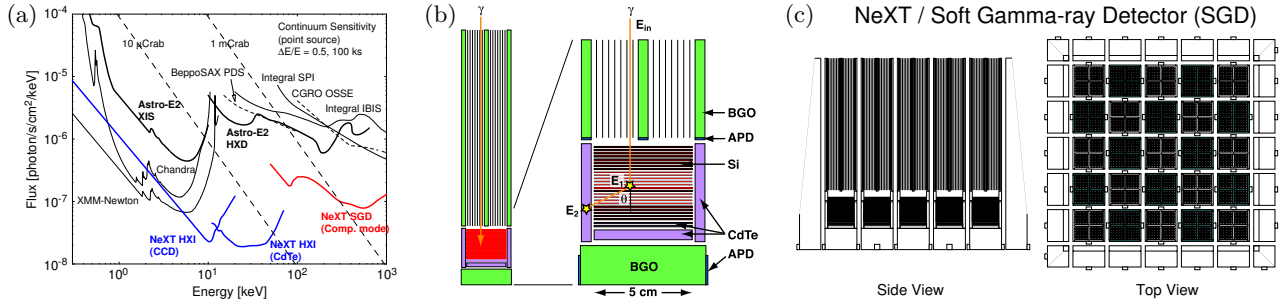

Figure 1: (a) Expected SGD sensitivities for continuum emissions from point source, assuming an observation time of 100 ks and comparison with other instruments. (b) Conceptual drawing of a SGD detector unit. (c) Conceptual drawing of the SGD instrument.

2. Instrument Description

The NeXT/SGD is a Compton telescope with narrow FOV, which provides a constraint on Compton kinematics to enhance its background rejection capabilities. The hybrid design of this module, illustrated in Figure 1 (b), incorporates both silicon strips (to enhance response below ∼300 keV) and pixelated CdTe detectors. The Compton telescope consists of 24 layers of DSSDs (double-sided silicon strip detectors) and 2 layers of thin (0.5 mm) CdTe pixelated detectors surrounded by 5 mm thick CdTe pixelated detectors. This arrangement is originated from a Si strip based Compton telescope proposed by T. Kamae *et al.* [5]. The DSSD strip pitch is chosen to be 0.4 mm to optimize the noise performance and power consumption. The DSSD thickness is 0.5 mm mainly to avoid the high depletion voltage while retaining moderate interaction probability. The pixel size of the CdTe detectors is 2×2 mm^2 to optimize the angular resolution of the Compton kinematics and the number of channels required. Thin CdTe detectors are placed underneath the DSSD layer to reduce the effect of the backgrounds as described in section 3. The size of DSSDs and thin CdTe detectors is approximately 5×5 cm^2.

A copper collimator restricts the field of view of the telescope to 0.5° for low energy photons (<100 keV), which is essential to minimize the CXB (cosmic X-ray backgrounds). A BGO ($Bi_4Ge_3O_{12}$) active collimator defines the FOV to 4° for high energy photons. A BGO bottom shield unit detects escaped photons and cosmic rays. Scintillation light from BGO crystals is detected by avalanche photo-diodes (APDs) allowing a compact design and low energy threshold compared with phototubes. The combination of a Compton telescope, BGO active collimator, a fine passive collimator constructed of copper and a BGO bottom shield forms a detector module that can detect photons in a wide energy band (0.05–1 MeV) at a background level of 5×10^{-7} counts/s/cm^2/keV. These modules are then arrayed to provide the required area. Figure 1 (c) shows a conceptual drawing of the SGD instrument, which consists of a 5×5 array of identical detector modules surround by BGO shield units.

We require each SGD event to interact twice in the stacked detector, once by Compton scattering in the Si or thin CdTe part, and then by photo-absorption in the CdTe part. Once the locations and energies of the two interactions are measured as shown in Figure 1 (b), the Compton kinematics allows us to calculate the angle between the telescope axis and the incident direction of the event using the formula,

$$\cos\theta \;=\; 1 + \frac{m_e c^2}{E_2 + E_1} - \frac{m_e c^2}{E_2}, \qquad (1)$$

where θ is the polar angle of the Compton scattering, and E_1 and E_2 are the energy deposited in each photon interaction. The direction of the incident photon can be confined to be on the surface of a cone determined from θ and the two interaction positions. The high energy resolution of the Si and CdTe devices help reduce the width of these "Compton rings". We can determine the location of point sources as intersections of multiple rings. The angular resolution is limited to ∼8° at 100 keV due to the Doppler broadening (assuming that the energy resolution is better than 1.5 keV), which is comparable to the FOV of the BGO collimators. Although the order of the events can be uncertain, we can use the relation that the energy deposition by Compton scattering is always smaller than that of the photo absorption for energies below $E_\gamma = 256$ keV ($E_\gamma = m_e c^2/2$). This relation holds above this energy, if the scattering angle θ is smaller than $\cos^{-1}(1 - m_e c^2/2E_\gamma)$. The major advantage of employing the Compton kinematics, however, is to reduce backgrounds. By having a narrow FOV, and by requiring the Compton ring of a valid aperture gamma-ray event to intersect with the FOV, we can reject most of background events. This dramatically reduces the background from radio-activation of the detector materials, which is a dominant background source in the case of the Astro-E2 HXD (Hard X-ray Detector) [6, 7]. Furthermore, we can eliminate Compton rings produced by bright sources located outside the FOV, which could produce significant background in some circumstances. It is crucial

to achieve low backgrounds since the photon sensitivity of the the HXD is limited by the backgrounds, not the effective area.

3. Background Suppression

Dominant background sources in the hard X-ray and soft gamma-ray bands are

- Source confusion and CXB (Cosmic X-ray Background)
- Cosmic rays and their secondary particles produced by the interactions with the satellite
- Internal background due to the contamination of long-lived radio isotopes in the detector material [7]
- Activation of the detector material due to the interaction with cosmic rays.

The first source can be minimized by limiting the FOV. The CXB is the dominant photon background source for the energy band less than 100 keV. To address this background term we implement a fine collimator, constructed of 50 μm copper arranged to provide a 30 arc-minute field of view. The FOV in the higher energy range is 4°.

The backgrounds due to cosmic rays and secondary particles can be suppressed by the active BGO collimator and shield.

The radioisotope contamination will be a dominant background source for the Astro-E2 HXD, which is the predecessor of the SGD and utilizes a similar well-type active shield configuration. The major contaminant is from ^{152}Gd in the GSO (Gd_2SiO_5) scintillator used in the HXD. The semiconductor devices we propose for use in the SGD are inherently free from any contamination. We still need to be concerned about the contamination in the BGO shields. Most of the background events emanating from the BGO shield are absorbed in the 5 mm thick CdTe detector and do not produce hits in the DSSD and thin CdTe layers. The self-background from the CdTe can be minimized by limiting the volume of the CdTe detector illuminated by the incident photons. Since the incident photons with energies less than 80 keV are absorbed in the thin CdTe layers, the activation background is suppressed by a factor of ∼5 by requiring an interaction in either DSSD or thin CdTe layers. Figure 2 shows the speactra of the self-backgrounds for 0.5 mm thick CdTe and 5 mm thick GSO. It clearly illustrates that the continuum background is reduced by more than an order of magnitude.

Further background suppression can be achieved by using the Compton events. In fact, most backgrounds can be rejected by simply requiring two hits (albeit with an attendant reduction in the instrument effective area). Applying the Compton kinematics and requiring consistency between the inferred incident photon direction and the FOV defined by the collimator will virtually eliminate the backgrounds from the bottom shield and CdTe detectors. The background from the BGO and copper collimator cannot be eliminated, but the source volume is small.

A background level of 5×10^{-7} counts/s/cm^2/keV is expected by employing these background suppression techniques, which is 20–100 times better than that of the HXD.

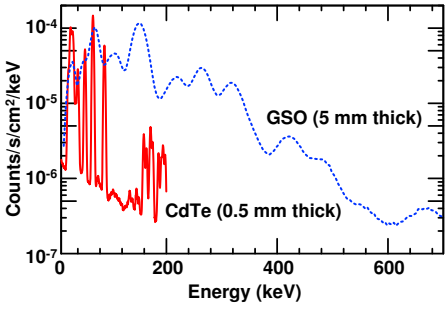

Figure 2: Spectra for GSO and CdTe activation backgrounds.

4. Expected Performance

The background level expected for the SGD is the key feature to achieve the sensitivity required to meet the science objectives of this project. In addition, the effective area must be maximized to detect sufficient number of photons for the observation of such faint objects in a reasonable amount of time. Figure 3 (a) shows the effective area as a function of the incident energy estimated using an EGS4 simulation. The solid curve represents the effective area with the absorption mode in which only total energy is measured without Compton kinematic constraint. Incomplete events are still suppressed by BGO anti-shield detectors. The dotted curve indicates the effective area with the Compton mode in which only events consistent with one Compton scattering and one photo absorption are accepted. The difference between the absorption mode and the Compton mode is due to zero-Compton scattering events in lower energy region ($E < 100$ keV) and multiple-Compton scattering events in higher energy region ($E > 100$ keV). Including multiple-Compton scattering events in the Compton mode can improve the effective area in the higher energy region.

Figure 3 (b) shows the expected energy spectrum for a 100 ks observation of 0.1–100 mCrab sources with the Compton mode. A background level of 5×10^{-7} counts/s/cm^2/keV is assumed. Figure 3

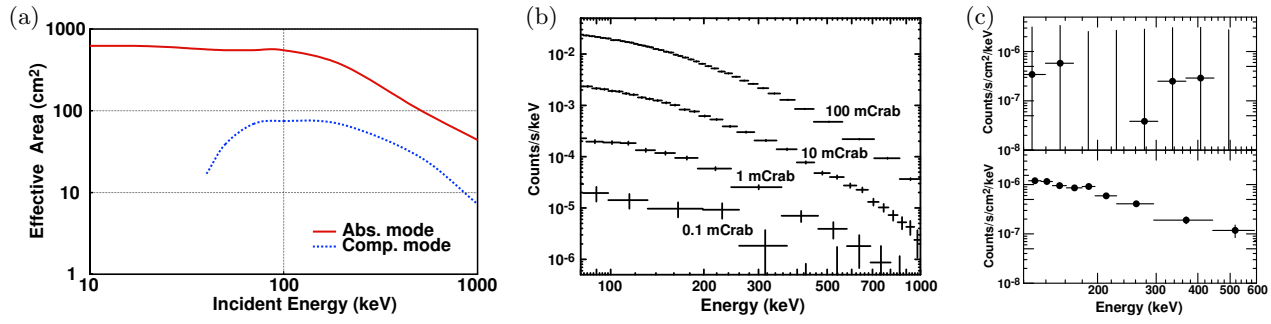

Figure 3: (a) Effective area as a function of incident energy for the absorption mode (solid) and the Compton mode (dotted). (b) Expected energy spectrum for a 100 ks observation of 0.1–100 mCrab sources with the Compton mode. A background level of 5×10^{-7} counts/s/cm^2/keV is assumed. (c) Comparison of the energy spectrum for a 100 ks observation of 1 mCarb source expected from the SGD Compton mode (bottom plot) and the instrument with the effective area of 3300 cm^2 and a background level of 5×10^{-4} counts/s/cm^2/keV (top plot).

(c) compares the energy spectrum for a 100 ks observation of 1 mCrab source expected from the SGD Compton mode (bottom plot) and that for the instrument with the effective area of 3300 cm^2 (50 times the SGD effective area) and a background level of 5×10^{-4} counts/s/cm^2/keV (top plot). It clearly demonstrates the importance of the low background.

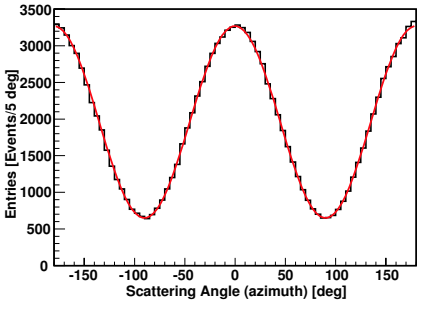

Figure 4: Azimuth angle (ϕ) distribution of the Compton scattering reconstructed for a 100 ks observation of a 150 mCrab source with a 100% polarization.

Figure 4 shows the azimuth angle (ϕ) distribution of the Compton scattering reconstructed for a 100 ks observation of a 150 mCrab source with a 100% linear polarization. The distribution is fit to a formula, $AVG \cdot (1 + Q \sin 2(\phi - \chi))$, where AVG is the average flux per bin, Q is the modulation factor which should be proportional to the polarization, and χ is the polarization phase and perpendicular to the polarization vector. The fit yields $Q = (66.89 \pm 0.30)\%$, which corresponds to the 5σ polarization sensitivity of 2.3%. Detailed studies of the SGD polarization performance can be found in [8].

5. Detector Performance Verification

5.1. Energy Resolution

High energy resolution is one of the key requirements for the SGD to retain a low background level with Compton kinematics. The energy resolution around 1 keV is required to approach the physical limit of the angular resolution due to Doppler broadening. We have developed a low noise front-end ASIC (Application-Specific Integrated Circuit), VA32TA, in collaboration with Ideas ASA in Norway to realize this goal. We have developed prototype modules for a low noise DSSD system in order to evaluate noise sources. To keep the strip yield close to 100% and eliminate polysilicon bias resistor (a possible noise source), the DSSD does not employ an integrated AC capacitor. We have produced 0.3 mm thick DSSDs with a strip length of 2.56 cm, a strip pitch of 0.4 mm and a strip gap of 0.1 mm. The C-V measurement indicates a depletion voltage of 65 V, therefore the following measurements are performed with a 70 V bias voltage. The leakage current is 0.5 nA/strip at 20°C and 0.05 nA/strip at 0°C. The strip capacitance is measured to be 6.3 ± 0.2 pF. Intrinsic noise performance with a silicon strip detector is measured to be 1.0 keV (FWHM) at 0°C, which is in good agreement with the analytically calculated noise value of 0.9 keV [9]. The energy resolution for γ-rays is investigated using the 14.4 keV and 122.06 keV γ-ray lines from ^{57}Co and the 59.54 keV γ-ray line from ^{241}Am. Figure 5 (a) shows the sum of the energy spectrum from ^{57}Co for all channels at -10°C. Fits yield energy resolutions of 1.1 keV (FWHM) for the 14 keV line and 1.3 keV for the 122 keV line [10]. Figure 5 (b) shows the energy spectrum from ^{241}Am at 0°C. A fit yields an energy resolution of 1.3 keV [9, 10]. The VA32TA performance for a CdTe detector is also evaluated using an 8×8 array of 2×2 mm^2 CdTe pixels. The thickness of the detector is 0.5 mm. Each pixel is connected to VA32TA via a fan-out board. Capacitance and leak-

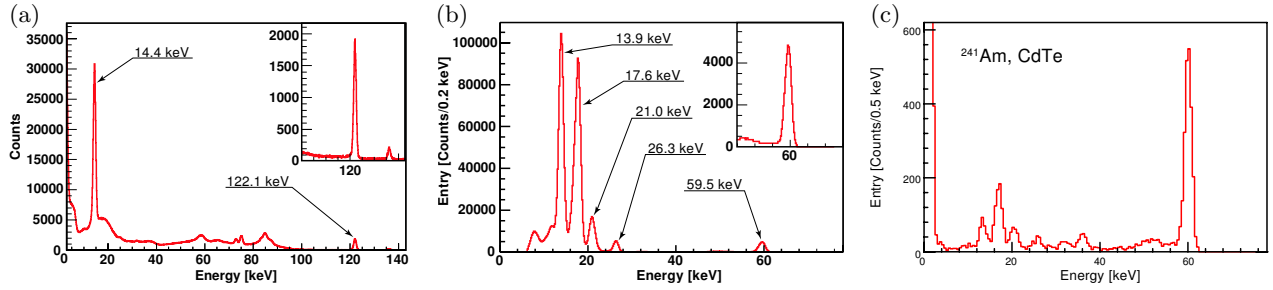

Figure 5: (a) Energy spectrum of ^{57}Co for a DSSD measured at -10°C. The 122 keV peak is magnified in the vertical axis in inset plot. (b) Energy spectrum of ^{241}Am for a DSSD measured at 0°C. The 60 keV peak is magnified in the vertical axis in inset plot. (c) The ^{241}Am energy spectrum for a CdTe pixel detector.

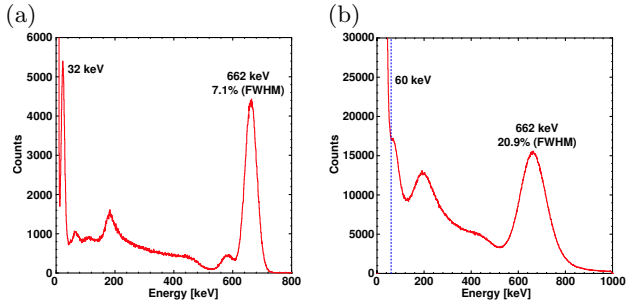

Figure 6: The ^{137}Cs energy spectrum (a) for a $10 \times 10 \times 10$ mm^3 BGO crystal with an APD readout at -20°C and (b) for a $300 \times 48 \times 3$ mm^3 BGO crystal with an APD readout at -15°C.

age current of each pixel are 1 pF and a few pA at 0°C. Low leakage current is realized by employing a guard ring to absorb leakage current from the detector edge [2]. Noise is measured to be 1.5 keV (FWHM). Figure 5 (c) shows the ^{241}Am energy spectrum at a bias voltage of 600 V. We obtain an energy resolution of 1.7 keV (FWHM) at 60 keV [9, 11].

The APD readout of BGO is a crucial part of the SGD detector development since it is extremely difficult to read out BGO collimators with phototubes due to mechanical constraints. Higher quantum efficiency of the APD will also contribute to lower the energy threshold of BGO. A large area reverse-type APD (10×10 mm^2), S8664-1010N, has been developed by Hamamatsu Photonics. The reverse-type APD can obtain sufficient internal gain at relatively lower bias voltage and low leakage current. The S8664-1010N achieves the internal gain of 50 with the bias voltage of ∼380 V at -20°C while keeping the leakage current at ∼60 pA [12]. We have evaluated the performance of this APD attached to BGO crystals. Figure 6 (a) and (b) show the ^{137}Cs energy spectrum with a $10 \times 10 \times 10$ mm^3 BGO block at -20°C and a $300 \times 48 \times 3$ mm^3 BGO plate at -15°C, respectively. The small BGO is attached directly to the APD while the large BGO is attached to the APD via a light guide. Energy resolutions are 7.1% (FWHM) for the small BGO and 20.9% for the large BGO [12]. Minimum detectable energies are 11 keV for the small BGO and 60 keV for the large BGO. Preliminary measurements with an array of eleven 3-mm diameter APDs achieved minimum detectable energies of ∼40 keV at -20°C and ∼20 keV at -40°C. We plan to develop an APD which closely matches the cross section of the large BGO plate to further improve the performance.

5.2. Compton Reconstruction

We have assembled a small prototype Compton telescope that consists of a DSSD and two CdTe detectors [13]. The DSSD and the CdTe detectors are placed in parallel with a distance of 12.5 mm. In this measurement, the telescope is exposed to ^{57}Co (122 and 136 keV) and ^{133}Ba (81 keV, 303 keV and 356 keV) sources to study the performance in wide energy range. Events with one Compton scattering in the DSSD and one photo-absorption in the CdTe are selected using Compton kinematics in a similar manner above. Figure 7 (a) shows the angular resolution as a function of the energy [13]. It also shows the Geant4 MC simulation estimates for the total angular resolution and contributions from Doppler broadening, energy resolution and position resolution. The Doppler broadening effect is the dominant source of the angular resolution up to 300 keV. The position resolution becomes significant in higher energy. Using the same data set, the effect of the background rejection by Compton kinematics is also studied. First, the energy spectrum is obtained for events with one hit in the DSSD and one hit in the CdTe. Then, the background rejection is applied by requiring $|\Delta\theta| < 16°$. Figure 7 (b) shows the ^{133}Ba spectra with (hatched histogram) and without the background rejection by Compton kinematics [13]. It clearly demonstrates that the effect of this technique. Note that the background rejection criteria are not optimized, and can be improved significantly, in particular in low energy region. Detailed description of Compton reconstruction studies can be found elsewhere [10, 13, 14].

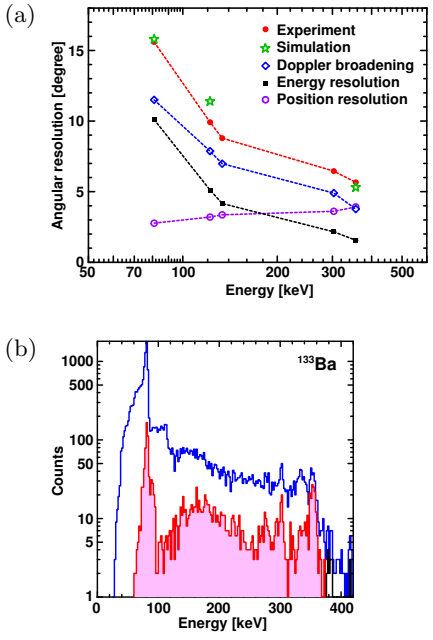

Figure 7: (a) Angular resolution as a function of energy for the experimental data and the MC simulation. Contributions from Doppler broadening, energy resolution and position resolution are also displayed. (b) ^{133}Ba spectra with (hatched histogram) and without the background rejection by Compton kinematics.

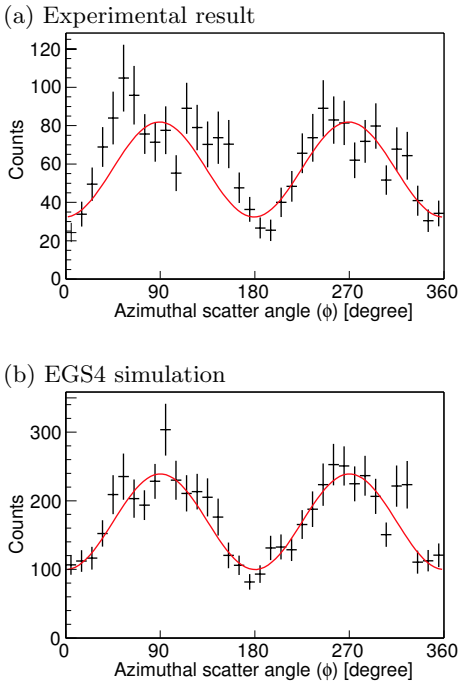

Figure 8: (a) Azimuth angle distribution of the Compton scattering obtained using a Compton camera consists of a DSSD and CdTe pixel detectors with 177 keV polarized photon beam at SPring-8. (b) Corresponding distribution by EGS4 simulation.

5.3. Polarization

In order to evaluate the polarization performance of the prototype Compton telescope, we have carried out a beam test at SPring-8 photon factory in Japan [11]. Figure 8 (a) shows the azimuth angle distribution of the Compton scattering obtained using 177 keV photon beam with a 100% linear polarization. Figure 8 (b) shows the corresponding distribution simulated by the EGS4 MC simulation. A fit on the experimental measurement yields the modulation factor of $43 \pm 3\%$ which is in a good agreement with the EGS4 result of $41 \pm 2\%$ [11]. These results validate our implementation of the EGS4 simulation at 10% level.

6. Conclusions

The NeXT/SGD is a Compton telescope with narrow field of view, which utilizes Compton kinematics to enhance its background rejection capabilities. It is realized as a hybrid semiconductor gamma-ray detector which consists of silicon and CdTe detectors. We expect the sensitivity of the SGD to reach 5×10^{-7} counts/s/cm^2/keV, allowing the observation of 1 mCrab sources in the energy range 0.05–1 MeV in 100 ks. We also expect 5σ polarization sensitivity of 8.7% for 10 mCrab sources.

We have developed low noise analog ASICs and CdTe detector technologies required to realize the SGD. We have achieved 1.1 keV and 1.3 keV energy resolutions for silicon strip detectors at 14 keV and 60–120 keV, respectively, and 1.7 keV for CdTe pixel detectors at 60 keV. We have verified that the APD readout of BGO crystal can detect the energy deposit down to 11 keV.

We have demonstrated the performance of prototype Si/CdTe Compton telescopes. MC simulations are validated against the experimental data on the angular resolution and the polarization performance. Doppler broadening is the dominant contribution to the angular resolution and the energy resolution, and position resolution is confirmed to be satisfactory. These experimental results validate the SGD design and specifications.

Acknowledgments

This work has been carried out under support of U.S. Department of Energy, contract DE-AC02-76SF00515, Grantin-Aid by Ministry of Education, Culture, Sports, Science and Technology of Japan (12554006, 13304014), and “Ground-based Research Announcement for Space Utilization” promoted by Japan Space Forum.

References

[1] T. Takahashi, K. Nakazawa, T. Kamae, H. Tajima, Y. Fukazawa, M. Nomachi, and M. Kokubun, "High resolution CdTe detectors for the next generation multi-Compton gamma-ray telescope," in *X-ray and Gamma-ray Telescopes and Instruments for Astronomy, SPIE*, J. E. Truemper and H. D. Tananbaum, eds., **4851**, pp. 1228–1235, 2002.

[2] K. Nakazawa, T. Takahashi, Y. Kobayashi, T. Mitani, T. Tanaka, K. Oonuki, G. Sato, S. Watanabe, R. Ohno, A. Kitajima, Y. Kuroda, and M. Ohnishi, "Improvement of the CdTe diode using a guard-ring electrode.," *IEEE Trans. Nucl. Sci.* **51**, pp. 1881–1885, 2004.

[3] T. Takahashi, A. Awaki, T. Dotani, Y. Fukazawa, K. Hayashida, T. Kamae, J. Kataoka, N. Kawai, *et al.*, "Wide-band x-ray imager (WXI) and soft gamma-ray detector (SGD) for the NeXT mission," in *UV and Gamma-Ray Space Telescope Systems*, *SPIE* **5488**, pp. 549–560, 2004.

[4] NeXT mission working group, "NeXT mission proposal (in Japanese)," Japan, November 2003.

[5] T. Kamae, R. Enomoto, and N. Hanada, "A new method to measure energy, direction, and polarization of gamma rays," *Nucl. Instrum. Methods A* **260**, pp. 254–257, 1987.

[6] T. Kamae, H. Ezawa, Y. Fukazawa, H. M, E. Idesawa, N. Iyomoto, *et al.*, "Astro-E hard X-ray detector," *Proc. SPIE* **2806**, p. 314, 1996.

[7] M. Kokubun, Y. Fukazawa, E. Idesawa, J. Kataoka, T. Kamae, K. Matsuzaki, T. Mizuno, Y. Saito, T. Takahashi, K. Takizawa, M. Tashiro, T. Tamura, and A. Yoshida, "Activation of the Astro-E hard X-ray detector in low earth orbit," *IEEE Trans. Nucl. Sci.* **46**, pp. 371–376, 1999.

[8] H. Tajima, G. Madejski, T. Mitani, T. Tanaka, H. Nakamura, K. Nakazawa, T. Takahashi, Y. Fukazawa, T. Kamae, M. Kokubun, D. Marlow, M. Nomachi, and E. C. Silva, "Gamma-ray polarimetry with Compton telescope," in *UV and Gamma-Ray Space Telescope Systems*, *SPIE* **5488**, pp. 561–571, 2004.

[9] H. Tajima, T. Nakamoto, T. Tanaka, S. Uno, T. Mitani, E. do Couto e Silva, *et al.*, "Performance of a low noise front-end ASIC for Si/CdTe detectors in Compton gamma-ray telescope," *IEEE Trans. Nucl. Sci.* **51**, pp. 842–847, 2004.

[10] Y. Fukazawa, T. Nakamoto, N. Sawamoto, S. Uno, T. Ohsugi, H. Tajima, T. Takahashi, T. Mitani, T. Tanaka, and K. Nakazawa, "Low noise double-sided silicon strip detector for soft gamma-ray Compton camera," in *High Energy Detectors in Astronomy*, *SPIE* **5501**, pp. 197–207, 2004.

[11] T. Mitani, T. Tanaka, K. Nakazawa, T. Takahashi, T. Takashima, H. Tajima, H. Nakamura, M. Nomachi, T. Nakamoto, and Y. Fukazawa, "A prototype Si/CdTe Compton camera and the polarization measurement," *IEEE Trans. Nucl. Sci.* **51**, pp. 2432–2437, 2004.

[12] T. Ikagawa, J. Kataoka, Y. Yatsu, T. Saito, Y. Kuramoto, N. Kawai, M. Kokubun, T. Kamae, Y. Ishikawa, and N. Kawabata, "Study of large-area Hamamatsu avalanche photodiode in a γ-rays scintillation detector," *Nucl. Instrum. Methods A* , 2004 (in press).

[13] T. Tanaka, T. Mitani, K. Nakazawa, K. Oonuki, G. Sato, T. Takahashi, K. Tamura, S. Watanabe, H. Tajima, H. Nakamura, M. Nomachi, T. Nakamoto, and Y. Fukazawa, "Development of Si/CdTe semiconductor Compton telescope," in *High Energy Detectors in Astronomy*, *SPIE* **5501**, pp. 229–240, 2004.

[14] S. Watanabe, T. Tanaka, K. Nakazawa, T. Mitani, K. Kousuke, T. Takahashi, T. Takashima, H. Tajima, Y. Fukazawa, M. Nomachi, S. Kubo, M. Onishi, and Y. Kuroda, "Si/CdTe semiconductor Compton camera," in *Proceedings of IEEE Nuclear Science Symposium*, 2004.